Reviews of Electromagnetics, Vol. IV, 2025
EuCAP 2025 Special Issue
DOI: 10.53792/RoE/2025/25020

Reviews of Electromagnetics
EuCAP 2025 Special Issue

Fast, Low-Invasive Visualization of EM-Very-Near-Field Distributions: from Anechoic Chamber to Microscope

Jean-Charles Bolomey[1]*, Manuel Sierra-Castañer[2]

Abstract
Fast and accurate visualization of Electromagnetic (EM) field distribution is satisfactorily obtained by numerical modelling. However, it still constitutes a key challenge in the case of measurements. The application of EM visualization covers a wide spectrum of demanding applications in wireless communications systems and sensing devices. EM visualization is an important tool in all the phases of the communications design steps: from the early design and prototyping of antenna modules to final on-line fabrication and compliance testing of mass-produced connected devices. In the last years, the measurement time has been drastically reduced thanks to several modalities exploiting either various interaction mechanisms between EM waves with adequate sensitive materials or the combination of standard Near-Field (NF) measurements with optimized sampling strategies and advanced wavefront post-processing techniques to retrieve Very-Near-Field (VNF) distributions. The aim of this extended paper is to provide an overview of these modalities and enable an initial assessment of their potential in terms of rapidity, sensitivity, invasiveness and spatial resolution.

Key terms
Antennas; electromagnetics; propagation; measurements; near-field visualization

[1] *University Paris-Saclay, Gif-sur-Yvette, France*
[2] *Information Processing and Telecommunications Centre, ETSI Telecomunicación, Universidad Politécnica de Madrid, Madrid, Spain*
***Corresponding author**: jeancharles.bolomey@gmail.com

Received: 25/05/2025, Accepted: 31/10/2025, Published: 04/12/2025

1. Introduction

Visualization has been the main process for developing the comprehension of our environment and the discovery of physical phenomena. Making the invisible visible has always been an exciting goal, all along the fundamental and innovative discoveries that have constantly paved the way for new applications. For example, in the visible spectrum, it is well the curiosity to see 'beyond the visible' that stimulated the development of optical instruments such as microscopes and telescopes, making it possible to observe things that, because of their size or distance, were beyond the natural perception of the human eye. The same need for visualization extends beyond the visible spectrum, to radio waves, given their raising prevalence in our daily lives and our growing dependence on them. The fact is that visualization is increasingly seen as an ideal tool for characterizing and fault diagnosing today's wireless communication and sensing devices, particularly those operating at frequencies ranging from microwave to millimeter and sub-millimeter waves. In these frequency bands, measurement methods must consider the impact of wavelength reduction on equipment dimensions. This dimensional aspect, which is directly correlated with the increase in bandwidth required to process an ever-increasing amount of data securely and with the lowest possible latency, has led to an evolution in both methods and technology. The usual black-box assembly approach of separately optimizing chip-package-PCB-antenna is abandoned in favor of a global optimization process of integrated antenna modules whose characterization techniques are challenging with existing measurement tools. The visualization of Very-Near-Field (VNF) distributions around or inside integrated circuits and antenna modules is therefore a promising area for investigation.

This paper is an extended version of the overview paper presented at the EuCAP2025 convened session "Fast, low-invasive

visualization of EM-VNF distributions around wireless communication/sensing devices: from anechoic chamber to microscope" [1]. It is by no means a comprehensive summary of the vast literature in this field. More modestly, its aim is, starting from a summary classification of the different approaches considered to date, to attempt of arriving, based on the available state-of-the-art, at their comparative potential in terms of rapidity, invasiveness, sensitivity and spatial resolution, with a view to future developments. The paper discusses advancements in electromagnetic (EM) wave visualization techniques, focusing on their application in wireless communication and sensing devices. It highlights the evolution of visualization methods from early attempts in the mid-20th century to modern approaches combining simulation, measurement, and multi-physics modelling. Key topics include experimental visualization scenarios, such as point-to-point EM-field probe measurements and global imaging using RF-sensitive materials, and their use in diagnostics, quality control, and compliance testing. The paper explores various visualization modalities, including Infra-Red Thermography (IRT), Fluorescence Thermography Imaging (FTI), Thermo-Elastic Imaging (TEI), Thermo-Reflectance Imaging (TRI), Nitrogen-Vacancy Center (NVC), and Rydberg Atom (RA) imaging, emphasizing their spatial resolution, sensitivity, and operational constraints. It also discusses the miniaturization of wireless devices and the resulting shared interest among antenna, EMC, micro-electronics and photonic communities in visualization as a multipurpose tool.

The paper is organized as follows. Sections 2 and 3 briefly explains the genesis of EM wave visualization approaches and suggests how they may be sorted in two major categories according to the selected 'shooting' imaging process. Section 4 is dedicated to the first, which is based on the formation of point-to-point images from results obtained from measurements made with manual, mechanical or electronic scanned RF probes. Then, Section 5, deals with different global imaging processes in which the EM field is visualized by its effect on a sensitive material acting as an indicator photographic plate. Such a promising approach transforming a field distribution into a full-scale or enlarged image visible with an optical or infrared camera, has the attractive advantage to use a 'one-shot' camerawork, but requires additional efforts to retrieve the full vector features of the EM field when needed. Finally, an overall comparison of the advantages and limitations of current visualization modalities is proposed, along with suggestions for promoting their use. The document concludes with discussions on the challenges of selecting appropriate visualization methods for specific applications, the need for comparative assessments, and the future of visualization technologies in education, research and industry.

2. Historical Revision of EM-waves Visualization

Attempts to visualize radio waves began with their discovery at the end of the 19th century (Fig. 1). The path followed since then has been complicated, and however, very stimulating facing the characterization of radiating devices, whether intended or not, mainly in the domains of Electromagnetic Compatibility (EMC) or as a support tool for antenna design. EM wave imaging only effectively emerged when radio wave operating frequency ranges reached the so-called microwave range for radar applications during the second world war. At that time, due to the lack of efficient computational tools, the design of radar antennas still relied heavily on measurements [2] and was mostly based on approximate and asymptotic formulations such as physical optics, equivalent aperture, and geometric diffraction theory. Additionally, the instrumentation available at the time would be considered very primitive by today's instrumentation standards, making difficult to afford the phase measurements, necessary for a proper use of Maxwell Equations.

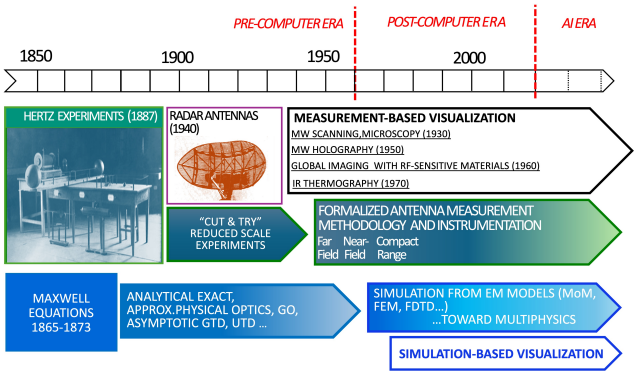

Figure 1: A simplified chronology of the development of EM-waves simulation and experimental methodologies and their correlation with visualisation, from their equation setting by Maxwell and their experimental validation by Hertz.

In the microwave range, the 'human-scaled' wavelength has clearly reignited interest in optical phenomenological and instrumental analogies, which were initially brought up prematurely at the discovery of electromagnetic (EM) waves but were later set aside during the early days of radio [3]. Among these optical analogies, holography [4], [5] and Scanning Near-Field Optical Microscopy (SNOM) [6], [7] are two examples of imaging-based measurement methods that have been successfully adapted from optics and are now recognized as part of the microwave visualization toolkit.

To accelerate these techniques, which can be time-consuming when they involve mechanical scans for data collection, the idea arose in the 1950s to use optical and/or infrared indicator materials that are sensitive to EM fields. These materials can function like photographic plates to visualize field distributions with sub-wavelength spatial resolution. However, despite its appeal, this concept of indirect global visualization, initiated a century earlier by Faraday's experiment (1851) on the visualization of magnetic flux lines produced by a permanent magnet using iron powder sprinkled on a wax-coated cardboard [8], has not yet fully concretized its promising potential or been accepted yet for routine practice, as shown in section 5.

On the contrary, directly extending standard EM-field measurement and simulation techniques toward visualization has led to significant advancements. Until the 1960s, experiment-based visualization primarily involved presenting measurement results as field profile cuts or radiation pattern plots, with little effort to create actual images. This changed when computers began to permeate the EM measurement and simulation fields, resulting

in two major impacts on visualization. Firstly, simulation, due to its flexibility and ability to handle complex configurations, quickly began to offer wave visualization in a comprehensive manner. Second, it spurred the development of Near-Field (NF) measurement techniques, which had long been hindered by heavy post-processing requirements to obtain the Far-Field (FF) radiation pattern, as well as by the lengthy duration of NF measurements process due to the mechanical scanning of the probe or the Device Under Test (DUT).

However, the combined effects of increased computer power and, in the late 1980s, a significant acceleration in NF data collection through probe array systems [9], solved, at least partially, the main drawback of the NF techniques, that was the long acquisition time. These techniques enable to retrieve radiated field distributions almost anywhere in space, even in the immediate vicinity of the DUT, from a minimal amount of NF data and within a reasonable timeframe, thanks to efficient wave-front transform post-processing [10]. As will be demonstrated in Section 4, the NF approach has progressively proven to be an effective means of achieving direct simulation-like, experiment-based visualization capabilities, with the invaluable benefit of working with real devices, whether they are intentionally radiating or not, thanks to usual available measurement equipment and modalities.

3. Different Approaches to VNF Visualization

Based on previous observations, VNF visualization approaches may be sorted in two major categories according to the selected 'image shooting' process. The direct approach is based on measuring the EM-field, while the indirect approach requires the prior use of sensitive indicator materials whose response must be translated into quantities related to the EM-field (Fig. 2). Before comparing the two approaches, it is worth recalling the general requirements to which they are subject as versatile functional and operational visualization tools that can be used in a wide range of applications, from the early steps of development of futures wireless devices to their final compliance/quality testing and maintenance. Firstly, these requirements are highly dependent on the characteristics of the DUT under consideration, particularly in terms of operational frequency band, transmitted power, dimensions, availability of access ports, to say a few. Secondly, for a given DUT, two distinct but complementary visualization objectives can be envisaged, namely characterization of the radiated field, on which the DUT final effectiveness depends, and/or detection and diagnosis of functional or structural faults, in its broadest sense, for instance during the antenna integration process in a module, or faults due to the EM measurement process. Thirdly, the degree of complexity of a visualization system is highly depending on the considered application and its performance requirements.

For instance, performance metrics may include rapidity (temporal resolution), invasiveness, spatial resolution, sensitivity, specificity, size and ease of integration of the visualization system into the operational DUT context, etc... states, this paper has deliberately focused on speed and non-invasiveness, as these appear to be two key elements to be considered for meeting the today practice visualization requirements for antenna measurement and EMC testing.

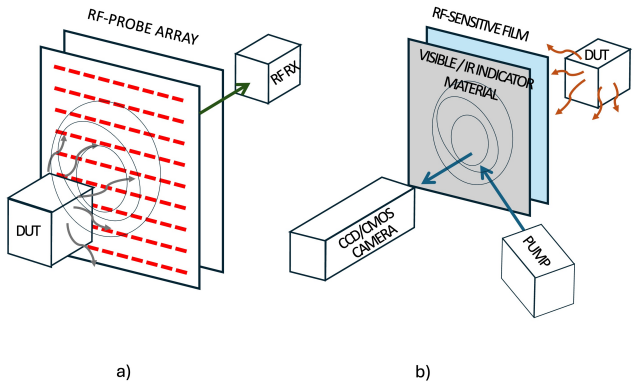

Figure 2: Principle of visualization arrangements: a) Direct approach using either a single probe mechanically scanned, or an electronically scanned multi-probe array connected to a RF-receiver, b) Indirect approach based on using a visible/IR indicator material activated by a RF sensitive film and read by a visible or IR camera.

Worth noting that, due to the operating frequency raise toward mm- and sub-mm wave and the resulting decrease of the dimension of wireless devices, the indirect visualization approaches are taking profit of the experience gained by visible and/or infrared visualization modalities already practiced for a while in IC fabrication processes. In other words, visualization of EM waves is becoming more than ever a field of research enriched by the fusion/combination of microwave and optical methods and technologies.

4. Direct EM-Field Visualization using RF Sensitive Probes

4.1. Early wavefront plotters

As already mentioned in Section 2, the lack of rigorous numerical tools for the design of reflector radar antennas has justified the need to precisely determine experimentally the position of the phase center of primary feeds, an essential issue for an accurate prediction of the FF pattern. While amplitude measurement was easily achieved with a probe connected to, whatever, quadratic detectors or superheterodyne receivers, phase measurement was the most based on an interferometric zero-method requiring manual or mechanical iterative and time-consuming adjustments of attenuator and phase shifter to ideally setup a perfect cancellation of probe and reference signals. The first attempt to speed-up the process was developed by RCA in 1947 which resulted in a so-called 'phase-front plotter' [11]. It consisted of a complex electro-mechanical recording arrangement using an E-field coaxial probe mechanically scanned, solidary of a stylus printing a current-sensitive paper sheet with a degree of darkening in proportion to the output of a quadratic detector submitted to the sum of the probe signal and of a phase-controlled reference signal. The complete record showing which parts of the scanned area have the same phase can be obtained within a few minutes, leading to the conclusion that *"such a record may really be said to be a picture of the radio*

waves...". In fact, it was, without telling it, probably the early microwave hologram recorder ever realized, even if not yet fully exploited as such. This early plotter system was later significantly improved, but complexified, for automatically drawing true amplitude and phase contours [12] leading to recognize it as the first NF antenna scanner [13]!

4.2. About probe invasiveness

The direct approach to the visualization of VNFs around a DUT consists basically of constructing, pixel by pixel, an image from the signal delivered stepwise by a single minimally invasive RF probe scanned in space around it (Fig. 3.a,b). A wide range of probes and measuring methods are available for this purpose and may be combined in various ways depending on the required compromise between speed and invasiveness. Probes are generally divided into 'metallic' and 'dielectric' probes. Metallic probes are nothing but small antennas such as dipoles, loops, waveguides, horns, etc. whose dimensions are minimized to reduce their invasiveness while retaining sufficient sensitivity and spatial resolution. Metal probes are generally connected to a receiver by a cable or waveguide which, together with the probe's mechanical support, increases their overall invasiveness. However, the invasiveness of metallic probes can be drastically reduced, if they are operated as scatterers according to the Modulated Scatterer Technique (MST) [14], [15]. The LF modulation of the load impedance of the probe (via low invasive resistive wires, or a laser beam) results then in a modulated scattered signal collected either by the antenna of the DUT itself, when possible (mono-static mode), or by a distinct auxiliary antenna (bi-static mode), as shown on (Fig. 3.b). Moreover, the modulation of the probe improves measurement immunity against non-modulated parasitic environmental scatterers.

On the other hand, dielectric probes, as their name suggests, are metal-free and are usually connected to the receiver via non-perturbing optical fibers. Instead of supporting electric currents, dielectric probes exploit the perturbation induced in indicator materials whose some physical properties (temperature, pressure, humidity...) are sensitive to EM wave exposure. The perturbation induced via classical, or quantum mechanisms is then detected via optical fibers or laser beams. For example, probes based on electro-optics effects [16], [17], [18], or on quantum technologies such as Rydberg atoms in vapor cells [19], [20], or Nitrogen Vacancy Centers in diamond [21], [22] offer, in addition to unrivaled minimal interaction with the DUT, high sensitivity and sub-wavelength spatial resolution capability. Recently, these complex technologies have been gradually made accessible for a simplified and competitive laboratory implementation, for EM field metrology and microwave imaging applications, for example [23], [24].

Single-probe scanning suffers from obvious rapidity limitations. However, in well-defined and accessible regions of interest, robot-controlled scanning of a dielectric probe may be efficiently used for fast and low-invasive visualization [25]. But even manual scanning may be also considered [26]. More particularly, using Augmented Reality headsets with only common sensor lab-equipment, has demonstrated its unrivaled efficiency and flexibility for fast hand-held in-situ visual spatial and frequency probing of EM field distribution, especially in complex environments, whatever closed or outdoor [27], [15].

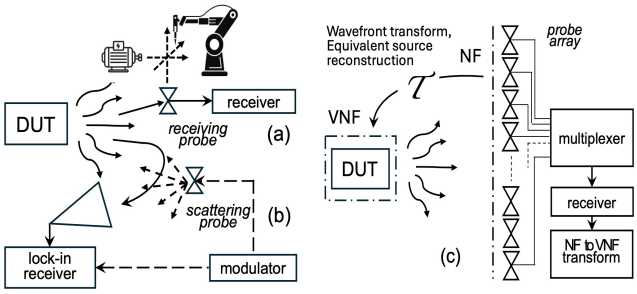

Figure 3: Principle of direct EM-field visualization arrangements: single RF probe manually or mechanically scanned: (a) receiving mode, (b) MST bi-static scattering mode (b) [15]; (c) electronically scanned receiving probe array with post-processing NF-to-VNF wave transform T.

4.3. Probes and probe arrays for antenna measurement

More generally, the rapidity issue has been addressed by considering solutions based on fast electronic scanning probe arrays (Fig. 3.c). But until the early 1980s, the simple idea of using an array of fixed probes remained completely unimaginable, on the argument that probe arrays would inevitably have introduced an unacceptable level of interaction with the DUT. However, this fatality was to be contradicted by a first generation of probe array. The first 'historical' probe array (Fig. 4.a) [28] consisted of a combination of small dipoles loaded by PIN diodes integrated into a frequency selective surface (FSS) panel incorporating the wires required for sequential modulation of the diodes. Furthermore, the panel was designed to be maximally transparent in a given frequency band when all the diodes are in the OFF state. Such a panel arrangement was part of an electromagnetic lens, coined Radant system [29], [30], developed to provide a low-cost alternative to expensive phased arrays beam scanning. Used as modulated probe array for NF measurements, this technology enables easy electronic probe scan via a simple LF multiplexer and offers the double advantage of rapidity and low invasiveness. The first proof of concept was obtained at S band with a monostatic MST setup involving a 3m x 1m Radant panel whose only one line of 115 dipoles was loaded with diodes, while all other dipoles were simulating an OFF state loading. The panel was optimized for 2.8-3.2 GHz operation with a quarter wavelength probe spacing and low invasiveness. At one wavelength distance of DUT's consisting of a horn antenna and 16x4 dipoles phased array, the NF measurement rate was 0.5ms/point, as compared to 10ms/point and 10μs/point, for electromechanical and electronic switches, respectively.

The rapidity and low invasiveness of this low-cost MST technology overcame preconceptions against the use of probe arrays and provided a springboard for the further development of antenna measurement systems, but not only. Indeed, without waiting for a sufficient increase of its sensitivity to rival the accuracy of single-probe NF antenna measurements, MST technology offered attractive camera solutions for less quantitatively

demanding detection applications. For these applications, the visualization objectives are no longer to characterize the field radiated by an antenna, but rather the field diffracted by the materials under study in order to reveal their internal structure non-invasively and specifically, when they are illuminated by a known antenna. Thanks to their real time visualization capability, the potential use of early MST-based microwave cameras in the GHz frequency for fast, non-invasive, and non-destructive fault detection and diagnosis has been widely investigated and exploited for various industrial and medical applications, e.g. [31]-[36]. Further improvement of sensitivity and specificity were obtained, both on hardware and software levels, for example through switched [37] or multiplexed [38] active probe arrays, and advanced image reconstruction algorithms [39].

Today, the concept of probe panels for sensing cameras is increasingly being addressed in the context of metamaterial absorbers [40], which are currently a very active field of investigation. The design of metamaterials offers the flexibility needed to meet application dependent requirements. Proper adjustment of multi-layer structures can balance sensitivity, invasiveness, and mutual coupling between probes. This results in high pixel density and sub-wavelength spatial resolution within specified frequencies [41], [42]. If panels of sensing cameras exploit metamaterial absorbers know-how, reciprocally, they may serve as an unrivaled investigation tool for characterizing basic interaction phenomena of EM waves with metamaterials [41],[43]. As a result, metamaterial absorber panels have a wide range of applications that require minimisation of reflected power, such as, for example, improving wireless energy transfer or radar target stealth [44].

As observed above for antenna NF measurements, the need to obtain sensitivity and accuracy comparable to those obtained with a single probe has led to the gradual replacement of MST probes by multiplexed probes. This led to consider moving from a panel of integrated probes to a modular assembly of independent probes. For example, the use of multiplexed Vivaldi-type probes has made it possible to both improve sensitivity and extend bandwidth, at the cost of increasing system complexity as well as measurement time and extending measurement distances to a few wavelengths in order to maintain an acceptable level of invasiveness.

A significant simplification of multiplexed probe systems was achieved by reducing the number of probes through hybrid setup arrangements. These setups combine fast measurements with linear or circular probe arrays, along with mechanical translation or rotation of the Device Under Test (DUT), to cover the surface to be scanned. For instance, circular probe arrays can be effectively employed for cylindrical or spherical coordinates by translating or rotating the DUT accordingly. Such circular probe arrays have been developed in fixed, transportable and mobile versions accommodating diameters ranging from 1 to 6 meters for applications in the wireless, aerospace and car industries. They find many applications for testing antennas, alone, integrated or in situ, across frequency bands from 70 MHz to 60 GHz with dynamic range of 50 to 70 dB. This fast hybrid NF concept has been validated thanks to a multicentre and multimodality evaluation campaign organized by EurAAP, sealing its perfect acceptance among long, compact and single probe NF antenna measurement ranges [45], [46].

Indeed, the potential of NF measurements is not only to enable the calculation of the Far-Field pattern of electrically large DUTs, their initial goal. NF measurements also enable to retrieve the radiated VNF, even in the vicinity of small antennas, thanks to the now well-controlled equivalent source retrieval algorithms [47]. The visualization of the equivalent current distribution offers a possibility to analyze and possibly reduce the interaction between a small on-chip antenna and its measurement setup, including mechanical support and the connected micro-probe required to feed it [48]. From only two tangent E or H components on a surface surrounding the DUT, the three E and H components can be determined thanks to wavefront transform or equivalent source reconstruction, offering so remarkable flexibility in terms of 3D visualization capability. Algorithms are available to process amplitude-only data. They are particularly beneficial in scenarios involving millimeter waves, where phase measurements can be challenging [49]-[53]. Additionally, as discussed in Section 5, these algorithms are required to translate temperature maps on thermal sensitive indicator materials into vector field distributions.

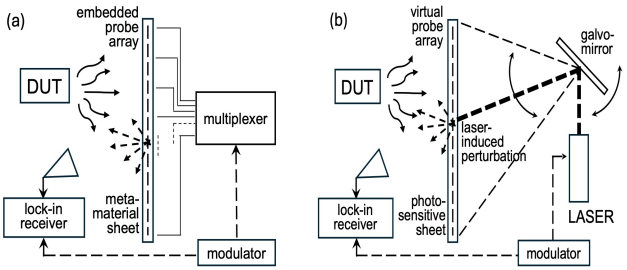

Figure 4: Examples of fast visualization bi-static modulated scattering-based setups: (a) array of modulated probes embedded in a meta material/FFS substrate [15]; (b) virtual array of photo-induced modulated probes [56].

Using photosensitive components as load of modulated probes has been considered as an option from the early days of MST to avoid any perturbation due to modulation wires [54], [55]. Fig. 4.b shows a recent innovative extension of this option involving a plasma induced 'virtual' probe array consisting in a photosensitive semi-conductor material sheet illuminated by a scanned modulated near-infrared laser beam [56]. The conductive spot in the semi-conductor induced by the laser beam behaves as a scattering probe whose mm-scaled effective area is determined by the beam cross-section. Scanning the beam results in remarkable mm-scaled spatial resolution and avoids any interpixel coupling [57]. For large DUT's, a multilayer matching approach may be used to reduce multiple reflection disturbance between the DUT and silicon wafer. Compared with a metasurface/FSS solution (Fig. 4.a), whose bandwidth is limited by matching requirements for low invasiveness purposes, the bandwidth of the virtual probe network extends from a few GHz to several hundred GHz [58],[59]. However, when it comes to translate measured data into vector EM field values, the virtual probe array loses its advantage due to a less formal definition of the induced currents for serving as probe structure.

This example provides a perfect transition with Section 5 dealing with indirect approach to EM wave visualization where a sensitive indicator material, here a semiconductor wafer, is used instead of a discretized set of probes.

Prior to concluding the discussion on direct methods utilizing rapid field measurements with probe arrays composed of metallic antennas, it is pertinent to examine dielectric probe arrays, which are expected to be less intrusive. For example, Electro-optic sensors (EOS), already prevalent in VNF mechanically scanned measurements, have been suggested as suitable candidates in several studies [25]. However, to the best of the authors' knowledge, these probes have yet to be effectively implemented as array elements. The scenario is distinct concerning quantum sensors. Specifically, Rydberg Atom (RA) arrays have been identified as a promising approach [60],[61], as evidenced by several related patents [62]-[65] on advanced photonic vapor cell manufacturing technologies expressly proposed for this application [65]. Moreover, since 2022, NIST has consistently publicized an RF camera project that utilizes RA probes as array elements. Despite this, current literature does not reveal yet examples of operational RA-based probe arrays. Conversely, diamond Nitrogen Vacancy Centres (NVC) technology has progressed from employing single diamond probes in mechanical scans [66] to integrating a diamond film system capable of real-time imaging at micrometer-scale spatial resolution, with a Field of View (FOV) covering several dozen square millimeters [67].

4.4. Probes and probe arrays for EMC/EMI and SI testing

The previous section focused on visualizing radiated electromagnetic fields, intentionally or not, outside the DUT. Differently, this section is considering the visualization of VNF in the close vicinity of the DUT and even more particularly inside, where they are typically guided rather than radiated. In contrast to antenna measurement, the DUT transmits signals and waves propagating in a structurally complex space, with dimensions that can range from very small to comparable to the wavelength, depending on the local operating frequency. Within the Device Under Test (DUT), the frequency spectrum can range from kilohertz (kHz) to tens of gigahertz (GHz). This variation is contingent upon the location of the test point within the sequence of the DUT's low-frequency (LF), intermediate-frequency (IF), and radio-frequency (RF) modules, as well as the direct current (DC) power supply connections. In such a situation, and especially at small probing distance, the VNF distribution is more dependent on the shape and the size of DUT structure than on the wavelength. The required resolution scale and probing distance to the DUT can then vary greatly, from a few centimeters for standard printed circuits to a submicron scale for chip components.

For PCB [68], [69] testing and diagnostics, VNF visualization offers several advantages. It provides high-resolution, real-time, and cost-effective methods to identify and address some shared EMC/EMI and related signal integrity (SI) issues. It allows for the detection of anomalies that cannot be identified by standard global S-parameter measurements. High-resolution analysis of VNF and current distribution images enables efficient localization of structural or functional faults, identification of 'hot spots' or areas with parasitic emissions producing interferences or cross-talks. It also allows for evaluating the effectiveness of design changes and PCB optimization efforts [70]-[74]. In addition to direct visual structural analysis, VNF measurement techniques pave the road to the reconstruction of equivalent sources in real-world scenarios. These scenarios are frequently challenging to model accurately through numerical simulations in that they often involve real-world complex in-band and out-of-band coupling mechanisms. The reconstructed currents provide detailed insights into these mechanisms and allow for their modeling and prediction of far-field emissions.

As usually, the dimensions of the probe result from a balance between sensitivity, low invasiveness, and the required spatial resolution. Mostly, probes consist of short electric dipoles and small magnetic loops, properly oriented for measuring tangential and/or normal components [75]-[78]. They may be operated in either a receiving or MST mode. Dielectric sensors connected with optical fibers to a receiver enable minimizing perturbations induced on the DUT. The spatial resolution of such probes is typically around 100μm but remains highly dependent on their dimensions and distance to the DUT. These probes enable to investigate various structures, such as microstrip lines, coplanar waveguides (CPWs), substrate integrated waveguides (SIWs), and multilayer PCBs. Related EMC/EMI or SI problems include impedance mismatch, crosstalk, ground-bounce, and common-mode currents near transmission line discontinuities like bends and slots. Visualizing them allows targeted design modifications, such as filtering or shielding, to be implemented to resolve these problems. For high-resolution sampling, miniature tip or electro-optic probes can be used with NF Scanning Microwave Microscopy (NSMM) systems [79]-[82]. These systems typically offer a spatial resolution of about a few ten nanometers, suitable for detailed structural imaging of MMIC components and circuits. With a single probe, the overall imaging time, including acquisition and mechanical scanning, varies from a few minutes to several tens of minutes.

To reduce mechanical scan time, using probe arrays has been considered since the early 1990s as a powerful, efficient solution for diagnosing and resolving EMC/EMI issues in PCB design. Probe array systems may cover broad frequency bands from 150 kHz to 8 GHz, ideal for ultra-high-speed PCB diagnostics [70]. They considerably reduce test times and perform spatial scans in less than a second, with resolutions as fine as a few millimeters. Typically, probe array consists of a two-dimensional grid of current-sensitive magnetic probes [71]. For instance, to cover a 40 cm square flat surface, the number of probes ranges from 1,000 to 1,600, with a cm-scaled sampling step. The loops are integrated into a multilayer printed circuit board (PCB) structure, with a ground layer situated beneath the top surface to shield the feed network from external interferences. Calibration processes are used to account for interaction effects of the probes, the feed network and the ground plane with the PCB [72]. The probes are typically cross polarized allowing them to detect currents directed along two orthogonal directions.

NF probe arrays of the previous sub-section, originally used for antenna measurements, arose from the need to determine

the FF patterns of electrically large antennas. It was not until later that they were used to retrieve equivalent sources on the DUT as well as its NVF distribution. On the contrary, the exact opposite approach was followed in the case of VNF probe arrays. They were initially dedicated to measure the EM-field in the close vicinity of the DUT and, only later, considered to possibly be used to determine its FF pattern. Depending on the application, this VNF based methodology has been shown to be possibly advantageously used for fast determination of FF pattern with satisfactory accuracy while requiring a very simple on-table setup [74],[83]. It may be also possible to translating VNF probe arrays either to cover larger surfaces or to improve spatial resolution, possibly until a few tenths of mm, thanks to reducing the sampling rate and proper image processing. Although this approach requires careful calibration to compensate for interactions with the test object, it should be noted that in some cases it was sufficient to place a simple absorber sheet between the probe array and the test object to obtain acceptable results. In summary, VNF visualization with a probe array appears as an effective tool for PCB testing and diagnostics due to their precision, cost-effectiveness, visualization capabilities, and adaptability to complex designs. As in case of antenna measurement, the possible arraying of low perturbing dielectric probes should deserve some clarification.

5. Indirect EM-Field Visualization using RF Sensitive Indicator Materials

5.1. Early photographic visualization systems

This section explores visualization as a "staring" imaging process, comparing it to optical instrumentation. It started in 1951 with the publication of an article in the Bell System Journal, which detailed a photographic technique for *"displaying spatial patterns of sound waves and microwaves"* [84]. This approach was based on the use of a small dipole probe loaded by a neon lamp whose brightness was in proportion with the power detected. The experiment had to be carried out in a dark room and the image of the probe was recorded by a fixed camera as the probe was moved in space over the desired surface. Anecdotally, such a forgotten visualization process has been recently updated by replacing the in-dark time-consuming mechanical scan of the luminescent probe with a real-time acquisition inside a 50cm side cube filled with an array of 16x9x13=1872 magnetic loops loaded with LEDs [85]. This network was used to visualize, with a 4 cm sampling step, the VNF power distribution generated by a wireless device antenna operating at 13.56 MHz. Would it be to say that the perspective of 3D probe arrays be now open to further research and development? The future will tell us... Coming back in 1955, another photographic approach was described in a paper entitled *"A New Method of Observing Electro-Magnetic Fields at High Frequencies by Use of Test Paper"* [86]. It was explaining how to utilize thermal effects caused by irradiating lossy materials with electromagnetic (EM) waves. It is interesting to note that it referred to *"... a simple method of observing electro-magnetic fields at high frequencies, which enables us to see the relative distribution at once, it will be very convenient to the development of the theory of high frequency circuits and to the design of radio machines and instruments and their parts."* The foresight of that time was remarkable! The test material used was a paper sheet soaked in an absorbing cobalt chloride solution. When placed in the area where the EM-field distribution was to be visualized, its color changed from pale rose to blue due to the temperature increase resulting from dielectric losses. This initial paper test method was followed by various others that differed in the type of paper and the observed effects, including polaroid [87], liquid crystal [88], and photochromic films [89], among others. However, despite their promising results, none of these early attempts made a significant impact at the routine practice level, likely due to the lack of commercially available sensitive paper materials.

5.2. Introducing IR as visualization modality

Without waiting for Hertz experiments, InfraRed (IR) sensing has continuously and considerably evolved since IR discovery by Herschel in 1800 [90]. From the first thermal sensors such as thermocouples and bolometers until to today's CCD and CMOS focal plane arrays (FPAs) used in IR cameras, its evolution has been driven by interdependent advances in materials, electronic technology and applications [91],[92]. Born from the need to filter sun light to avoid eye burning during astronomical observations, the rapid growth of IR technology resulted from its ability to enable seeing what was escaping to human vision. As with microwave radar applications, the development of IR imaging was accelerated during the Second World War by defense applications to see enemy targets on the battlefield through the darkness of night or smoke. Elimination of the need for cryogenic cooling and further advances in silicon microelectronics resulted in a technological breakthrough enabling low-cost, high-performance sensors [93]. Hence IR imaging gradually moved from niche military tools to widely used technologies in civilian markets such as non-invasive material testing [94] or medical diagnostic imaging [95]. FPAs appeared in the 1970s, enabling true "staring" mode imaging without mechanical scanning. Finally, integration of read-out circuits with Charge-Coupled Devices (CCDs) and later CMOS technology allowed the development of fast, high-resolution, two-dimensional arrays with millions of pixels [96]. Current efforts continue to focus on increasing pixel density (over 1 million pixels), multi-spectral capabilities and intelligent sensors with integrated signal processing.

5.3. EM-Infra-Red thermography

In addition to the first photographic evaluations using thermal paper, briefly described in Section 5.1, the electromagnetic (EM) and thermal (TH) visualization technologies were combined more and more effectively from the mid-1970s because of their complementarity. IR Thermography (IRT) [97]-[100] emerged as a preferred method for mapping the fields radiated by microwave antennas [101],[102] or currents on conductors [103] or leakage sites in IC's [104]. In addition, due to their specific advantage over IR in terms of penetration into materials or biological tissue, microwaves have also begun to be exploited for passive industrial detection and medical diagnostic applications, just as it has been done previously with IR imaging. Fig. 5.a shows a basic planar IRT setup comprising a sheet of absorbing material, either continuously spread or pixelized,

placed close to the DUT. When exposed to EM wave radiated by the DUT, the power absorbed by the sheet results in a local increase of temperature proportional to the power radiated by the DUT. To minimize the effects of the thermal environment, a lock-in technique [104]-[106] is commonly employed, consisting in synchronizing the camera with a signal modulating, typically ON-OFF, the DUT. Such a modulation enables to isolate the temperature increment (ΔT) caused exclusively by the DUT, without considering environmental factors, while also minimizing unwanted image distortions resulting from thermal conduction and convection in the absorbing sheet. As a result, ΔT maps pictured by an IR camera can be correlated with the local dissipated power density and hence to the distribution of electric or magnetic VNF intensity radiated by the DUT. The correlation factor depends on the dielectric permittivity and/or magnetic permeability of the absorbing material as well as on its thermal properties and thickness. These factors impact must be accounted for optimizing of the lock-in modulation signal frequency with respect to sensitivity, rapidity and spatial resolution requirements [102]. The spatial resolution of such an EM-IR thermography system depends not only on the operating wavelength of the camera (usually in the Near IR) and the size of its FPA pixels, but also on the absorbing material. Indeed, governed by heat equation, the temperature information captured by a given camera pixel is in global intensity relation with other pixels rather than an intensity of single pixel. The temperature impulse response (Point Spread Function) was shown to be approximately look as a bidimensional Gaussian expression. The temperature PSF may be either measured or predicted thanks to EM-Thermal multi-physics codes. Such codes may be also usefully exploited to assess the degree of interaction of the absorbing sheet with a given DUT and, possibly, to compensate for the PSF spreading thanks to proper calibration. They also can be used to suggest how maintaining acceptable interactions and conduction or convection effects. Typically, IRT offers a spatial resolution in the few microns scale which, any way remains largely sub-wavelength at the operating wavelength of the DUT.

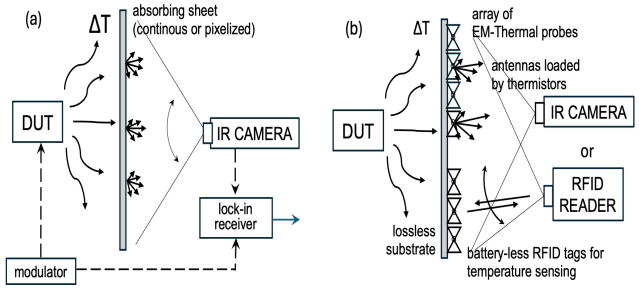

Figure 5: Thermal-based EM field sensing setups using: (a) an absorbing sheet as temperature indicator ; (b) an array of small thermal probes, antennas loaded by thermistors [107] or RFID tags equipped with thermometers [109].

To improve the sensitivity, pixelized screens have been proposed, each pixel acting as a materialized thermal sensitive probe. Fig. 5.b shows two examples of EM-Thermal probe arrays consisting of small metallic antennas loaded by a thermal-sensitive components and mounted on a loss-less and thermally insulated substrate. In the upper case Fig. 5.a, the component is a resistor, whose thermal emission is visualized with an IR camera [107], The array structure and the antenna dimensions are considered as a meta-surface and optimized to maximize the power collected by the antennas [108].

In the bottom case Fig. 5.b the probes consist of RFID tags loaded with integrated micro-thermometers and wirelessly connected to an RFID reader [109],[110]. Such a probe array is dedicated to medical hyperthermia treatment of superficial tumors. It consists of a dual-frequency band meta-surface enabling both microwave heating at 414MHz and temperature sensing at 913MHz. The structure is flexible and can fit the body part to be treated by hyperthermia. In this application, the aim is not so much to characterize the field radiated by the DUT inside the body to be treated as to measure its global effectiveness based on the map of the surface temperature for which it is responsible, by comparison with desired map obtained at the outcome of an optimized treatment planning via multiphysics modeling.

Similarly, IRT has been primarily used for diagnosing and detecting faults in antennas and circuits [111],[112]. Temperature maps can reveal and localize not only structural anomalies in passive components but also malfunctions in active circuits, as many potential defects directly affect temperature. Although translating ΔT into vector EM field distributions may not be straightforward, IRT has also been utilized for NF and FF pattern measurements [113]-[116], thanks to various post-processing based on holography and plane-to-plane iterative techniques that enable retrieval of EM field phase and polarization [117],[118].

The main advantages of IRT include its low invasiveness, speed, ease of operation, and the ability to provide micron-scale sub-wavelength spatial resolution. In contrast to traditional electromagnetic (EM) probes, which may cause distortion in the measured field due to metal components, cables, and mechanical supports, IRT offers the advantage of delivering relevant heat maps almost instantaneously, similar to capturing an optical image on photographic film.

However, the low invasiveness of IRT sheets, designed to minimize backscattering towards the DUT while maintaining acceptable sensitivity, results from optimizing the overall reflection, absorption, and transmission budget based on specific application requirements [119]. Sensitivity remains a challenge for IRT, as it requires the DUT to emit power in the watt range, either independently or with an external generator if accessible.

5.4. Other thermal based imaging systems

Over the last decade, other thermal based imaging modalities have been promisingly developed to overcome IRT limitations. Due to the dimensional aspects resulting from the increased operating frequency of wireless devices and the integration of antennas with RF/IF circuits in the same module, some of these methods are derived from those used for IC and chip manufacturing technology [104]. For antennas and circuits, temperature maps can be used to verify satisfactory operation through their dependence with respect to field strength and currents, while detecting unexpected hot spots can indicate functional abnor-

malities. These EM-Thermal visualization modalities exploit the temperature sensitivity of Optical Indicator (OI) materials when exposed to EM wave. These materials enable translating EM-induced temperature maps into visible images using optical cameras or microscopes, achieving sub-wavelength spatial resolution at DUT's operating frequencies.

Unlike Infrared Thermography (IRT), which is a passive imaging approach, these thermal-based methods are active. They require the OI material, typically a thin sheet or a coating, to be illuminated by a visible light source to stimulate its thermal sensitivity and make its effects detectable through the reflected light. The wavelength of the reflected light can be either the same or different from that of the incident light.

Temperature-dependent effects, such as thermo-fluorescence, thermo-elasticity and thermo-reflectance, are being increasingly explored for NF and VNF visualization all throughout the chip-package-PCB-antenna development line. These imaging techniques have demonstrated their feasibility in various DUT dimensions and frequency bands. Depending on the considered specific application active imaging offers a wide range of visualization solutions, from full-scale down to microscopic scale.

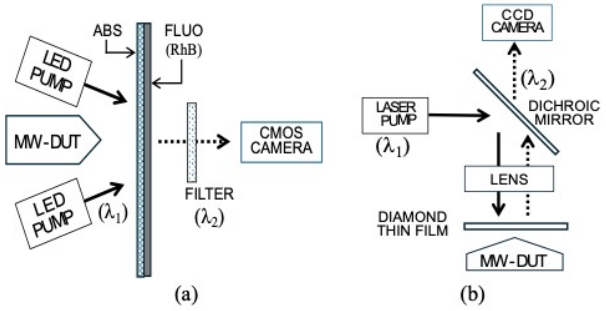

Figure 6: Schematic experimental setups for thermo-fluorescence imaging using optical indicators: (a) Rhodamid B (RhB) fluophore coating for transmission arrangement (λ_1=530nm, λ_2 around 600nm) [121]; (b) NVC Diamond thin film are used as optical indicator in a reflection-based microscopic arrangement [126].

5.4.1. Thermo-fluorescence imaging

In this sub-section, two different experimental arrangements are described. The first one shown on Fig. 6.a enables to perform large-scale imaging of the electric or magnetic field intensity as well as local temperature measurements. The wave transmitted by the DUT is illuminating the OI which consists of an absorbing screen coated by a thin fluophore-doped layer coating. The OI is also symmetrically illuminated by the light of two LED's at a wavelength λ_1 (around 535nm) well-suitable for exciting the Rhodamid B (RhB) fluophore coating, selected for its advantages in terms of quantum efficiency and spectral separation between absorption and emission spectra [120],[121].

A portion of the LED light is absorbed by the film and excites the fluorophore layer. The transmitted light is then captured by a CMOS camera after being properly filtered to retain a wavelength of approximately 600nm, which is close to the peak of the RhB fluorescence spectrum.

Such measurement setups enable acquisition of high-resolution maps (several megapixels) within seconds for low-invasive visualization of VNF distribution of DUTs such as broadband fractal [121] or X-band transmittarray antennas [122]. Because of their large area of investigation (around 50cm x 50cm), their wide frequency ranges from kHz to THz and their reasonable power requirement (a few watts), these devices look as practical and versatile low-invasive tool for qualitative antenna analysis, fault detection and diagnosis of antenna. If necessary, quantitative results may be obtained thanks to proper calibration. Like for IRT, only VNF intensity is directly accessible, but further post-processing can be used for phase retrieval and FF calculation. Last but not least, especially for educational purposes, worth noting that the cost of a visible CMOS camera is significantly smaller compared to that of an IR camera.

Fig. 6.b shows a second quite different option for an experimental arrangement now exploiting OI materials based on quantum magneto-optic effects. Optically Detected Magnetic Resonance (ODMR) is one of these effects which has been a rapidly growing branch of quantum technology aiming to exploit the fragility of quantum states for detecting small external signals with high sensitivity. More particularly, Diamond Nitrogen-Vacancy Centers (NVC), as a defect with microwave manipulable spin state and optical readout at room temperature, have attracted much attention for high resolution and sensitive microwave near-field characterization. During the past decade, the potential of scanning low-invasive single, sub-millimeter-sized, probe was demonstrated for characterizing 3-D microwave field distribution with microscale resolution [123] or even nanoscale [124]. Several papers have been devoted to investigating the potential of NVC miniaturized sensors and data processing for magnetic VNF measurements around MMIC's or antennas in S-band [125],[126].

A significant advancement was recently made by employing millimeter-sized square diamond chips as probes along with a CMOS camera. This technique enables the prevention of any displacement in the system structure and facilitates rapid visible imaging of MW field distribution, thereby ensuring high time efficiency and stability. The principle of a reflection visualization system based on this concept is shown on Fig. 6.b. Such an arrangement was used to visualize the magnetic field around a 100 micrometers radius wire antenna, in the 2.7-3.2 frequency band [127]. The spatial resolution was about 3μm with a FOV 5mm x 5mm and a power level about 0.8W. As compared to scanning microscopy solution, the gain in rapidity is significant, at the cost of lower spatial resolution. As compared to the previous Rhodamid B option, the sensitivity is better at the cost of a smaller FOV. A further advantage is that, instead of the magnetic field intensity, it is possible to measure its amplitude thanks to a synchronous pulsed sequence combined with the CCD. A full reconstruction formulation of the local field vector, including the amplitude and phase, is developed by measuring both left and right circular polarizations along the four nitrogen-vacancy crystalline axes [128].

5.4.2. Thermo-elastic imaging

Thermo-Elastic Optical Indicator Microscopy (TEOIM) is regarded as another promising high-resolution visualization tech-

nique. It employs polarized light microscopy to visualize the electromagnetic near-field distribution across a broad spectrum of operating frequencies. Fig. 7.a shows a typical TEOIM setup. The OI is composed of a slide glass substrate coated by a thin Indium-Tine-Oxide (ITO) film absorbing the magnetic field of the DUT. The heat generated in the ITO film diffuses into the thermo-elastic glass substrate, resulting in a thermal stress photo-elastic effect. The circular polarization state of the incident LED light (typ. λ_1=530nm) changes, after specular reflection, into an elliptically polarized state to be analyzed by a polarimetric microscope equipped with a CCD camera. Proper image processing enables retrieving temperature, magnetic field and electrical currents [129],[131].

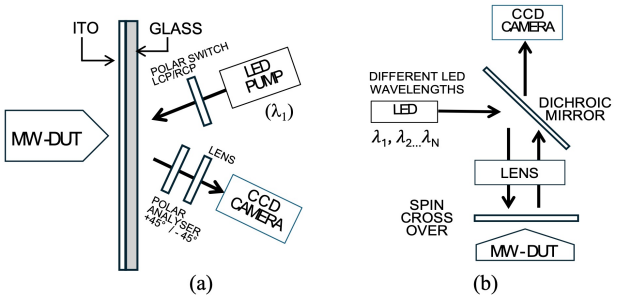

Figure 7: Schematic experimental reflection setups for thermal imaging using optical indicators: (a) Indium-Tint-Oxide (ITO) for thermo-elastic polarimetric microscopy arrangement [129].; (b) Spin Cross Over (SCO) coating for multi-spectral thermo-reflectance imaging.

TEOIM has been demonstrated to provide optically resolved temperature, electric, and magnetic microwave VNF images selectively with a comparable sensitivity, response time, and bandwidth of existing methods. It is considered as a practical investigation tool for various applications such as non-contact thermal imaging of PCB circuits [129], VNF imaging of antennas [131],[132] in the 0.1 to 10 GHz frequency range, with a field of view up to 5 cm x 5 cm. Its low invasiveness enables measurements at millimeter-scaled distances and DUT power levels in the Watt range. TEOIM systems seem particularly well-suited for studying the interaction phenomena between electromagnetic waves and metamaterials [133], with a focus on their structural characterization and optimization. This approach facilitates the development of improved designs and enhanced functionalities.

5.4.3. Thermo-reflectance imaging

The principle of a Thermo-Reflectance Imaging (TRI) system is shown on Fig. 7.b. Its looks like a free-space reflectometer where the incident light is provided by a LED source while the reflected light is observed with a CCD camera after proper focusing with a microscope. The image provided by the camera is a map of the reflection coefficient on the plane over which the system is focused. The focusing can be manually achieved either on a thermal optical indicator film or directly on the DUT itself generally consisting of metal and/or semi-conductor regions. In both cases, TRI exploits the temperature dependence of the local reflection coefficient. Like for IRT, the temperature increase T due to the DUT can be isolated thanks to a lock-in method consisting of synchronizing the camera exposure with the DUT modulated excitation. The operating wavelength must be selected in Thermo-Reflectance microscopy has been initially developed to be utilized by device manufacturers as a high-resolution non-invasive technique for quick failure analysis and temperature profiling of the devices under operating conditions [134]. Modulated thermo-reflectance set-ups and scanning thermal microscopy provide nano-meter and micro-meter scale thermal metrology[135]-[137]. In some cases, thermal images can serve as complementary information to the traditional electrical device test. Thermo-reflectance imaging is routinely used for IC and micro-electronics technology [138],[139].

Beyond small circuit imaging, thermo-reflectance has been considered as a holistic Near-Field (NF) visualization and testing solution for Chip-Package-PCB-Antenna modules based on combined thermo-reflectance and thin-film coating using Spin-Crossover (SCO) materials. The unprecedented quality of the SCO coating process exhibits highly reliable thermometric performance with diffraction limited sub-m spatial, sub-s temporal and 1°C thermal resolution [134]. In addition, the resulting performance qualifies the SCO coating process, in terms of fabrication and switching endurance (surpassing 107 thermal cycles in ambient air), for industrial testing ensuring highly reproducible measurement results. Such sensing solutions have been validated through several practical applications using front-end modules manufactured in advanced technologies co-designed with antenna-in-package (AiP) modules [140]-[142].

6. Opening Discussion and Conclusion

The measurement and visualization of electrical and magnetic fields has been an important task in the big scope of instrumentation, measurement, and education for many years as it enables a better understanding of physical phenomena. Fast recording of microwave field distributions remains an interesting approach for several scientific and engineering fields including the investigation of field radiation in terms of antenna design, EMC testing and of course educational purposes.

This overview paper has covered a wide range of modalities that enable the visualization of electromagnetic (EM) wave distribution, both around and inside wireless devices. These methods can be used directly or indirectly—through thermal signatures or other similar effects—to analyze the VNF (Very Near Field) distribution. The primary goal of these modalities is to characterize the radiated field itself or to detect potential faults, thereby offering diverse and valuable applications in the ongoing development of wireless devices. Beyond promising proof-of-concept demonstrations, some imaging systems have already achieved commercialization levels suitable for various industrial needs—from early product prototyping to final quality control—and are also fundamental tools in EM wave education and research.

Due to the difficulty of a quantitative comparison of so different methods, we are limited to show a qualitative description of the advantages and limitations of each family:

Classical direct EM-Field visualization using RF Probes

have the main advantage of the sensitivity and the matureness of the technology. However, the resolution is limited by the probe size, and, if some source reconstruction methods are used, it would be possible to get a resolution in the sub-wavelengths (the exact resolution depends on the method). The use of multi-probe allows to speed up the acquisition processes, but making more complex the RF system, including switching networks. Metamaterials is a promising technology for solving some of the issues of these multiprobe systems at frequencies above 100 GHz. With these methods, we have direct access to the electric or magnetic field.

Indirect EM-Field Visualization techniques require the measurement of another physical parameter; therefore, it is required a conversion between EM signal and this new physical parameter (i.e. temperature). This paper has analyzed the use of photographic, infrared, thermography, thermo-fluorescence, thermo-elastic and thermos-reflectance films. These techniques, which are stemming from optics or infrared frequencies, have been already extensively used in micro-electronics for detection diagnosis of IC (integrated circuits). The main advantages of these techniques respect the RF probes are the speed, allowing almost real-time acquisition, and sub-wavelengths spatial resolution due to optical read-out. Some of the problems of these techniques is that you lose information of the phase and polarization. There are some techniques (hardware and software) to reconstruct phase and modulations, at the cost of significant complexity of the systems. In this family, we can include the new quantum technologies, like the use of Rydberg Atoms or NVC sensors. These technologies are not yet mature enough, but they should improve very fast in the next years.

Current efforts in direct imaging should now focus on minimizing the invasiveness of probe arrays. The potential use of EOS (Electro-Optic Sampling) and Rydberg Atom technologies—pending confirmation of their cost-effectiveness—represents a significant advancement, thanks to their high sensitivity, spatial resolution, and adaptability to various modulated signal waveforms. Additionally, research into metamaterials should be continued, aiming toward the ultimate goal of achieving fully invisible cloaking [143].

Indirect thermal-based VNF visualization faces multidisciplinary challenges that go well beyond the traditional expertise of antenna and EMC communities. Close collaboration with materials science and solid-state physics is essential to develop comprehensive multi-physics simulation capabilities. These are crucial for validating experimental procedures, determining the best methods for translating temperature maps into field or signal information, and moving beyond mere visualization. Instead, machine learning techniques could be employed to diagnose faults by correlating local field deviations with temperature anomalies.

In this sense, the use of machine learning and artificial intelligence techniques are being developed for different applications in antenna design processes. Reference [144] is a very complete review of the possibilities of integrating artificial intelligence (AI) and machine learning (ML) techniques into the optimization and measurement of antenna designs. This review examines the latest advancements in applying AI/ML approaches, exploring several algorithms such as neural networks, decision trees, genetic algorithms, and particle swarm optimization, highlighting their potential, challenges, limitations and future research ways. This review concludes that AI/ML approaches have the capacity to transform antenna optimization and measurement processes by offering quicker and more precise solutions to complex problems. The use of AI/ML can be applied in the same way to all the visualization techniques, being able to improve the quality of the processed results and the speed of the EM field acquisition.

The relative novelty and promising prospects of visualization modalities for the characterization and diagnostics of wireless devices suggest that they merit consideration as a future open research area for the antenna design and measurement communities. It would be beneficial to focus research efforts and promote realistic proof-of-concept studies by: i) identifying applications with practical relevance, ii) establishing qualitative and/or quantitative performance criteria, and iii) conducting multi-modality comparison campaigns using available operational prototypes.

Currently, based on the state-of-the-art, it remains challenging to accurately assess the impact of different visualization modalities and determine their optimal application fields—whether used individually or as complementary tools. However, targeted optimizations can be envisioned to address specific needs related to speed, invasiveness, sensitivity, and spatial resolution. These improvements could enable VNF measurements around or inside wireless devices with sufficient accuracy to reliably diagnose failures in real time.

The application for new antenna systems, including reconfigurability, adaptive antennas or massive MIMO, among others, where there is not clear separation between antenna, RF subsystem, and digital processor, is direct. In these new antenna technologies, there is not a unique radiation pattern, but different ones depending on the value of amplitude and phase for each element in the case of the analog active arrays, or even infinite cases depending on the adaptive weights assigned by the signal processors in the adaptive arrays or massive MIMO scenarios. Therefore, the quality of the AUT should be evaluated using the extreme near field in the antenna aperture [145].

Finally, combining some of the techniques discussed in this paper with emerging approaches based on artificial intelligence could significantly accelerate antenna and device measurements—potentially enabling real-time analysis.

Acknowledgment

The authors would like to express their gratitude to all the authors involved in the EuCAP2025 convened session: ”Fast, low-invasive visualization of EM-VNF distributions around wireless communication/sensing devices: from anechoic chamber to microscope.

References

[1] J.Ch. Bolomey, M. Sierra-Castañer, “Fast, Low-Invasive Visualization of EM-Very-Near-Field Distributions around Wireless Communication/Sensing Devices: From Anechoic Chamber to Microscope”, European Conference on Anten-

nas and Propagation (EuCAP2025), Stockholm, April 7-11, 2025.

[2] S. Silver, Antenna Measurement, Chap.12, in "Microwave Antenna Theory and Design", Vol. 12, MIT Radiation Laboratory Series, McGraw Hill, 1949.

[3] J. F. Ramsay, "Microwave Antenna and Waveguide Techniques before 1900", in Proceedings of the IRE, vol. 46, no. 2, pp. 405-415, Feb. 1958, doi: 10.1109/JRPROC.1958.286869

[4] R.K. Amineh, N. K. Nikolova, XX? Ravan, "Microwave/Millimeter Wave Holography Based on the Concepts of Optical Holography," pp.17-32, chap.2 and "Microwave/Millimeter-Wave Holography for Near-Field Imaging Applications," pp.63-117 (chap.4) in Real-Time Three-Dimensional Imaging of Dielectric Bodies Using Microwave/Millimeter Wave Holography , IEEE 2019, doi: 10.1002/9781119538875.

[5] G. Tricoles, N.H. Farhat, "Microwave Holography: Applications and Techniques," Proc. IEEE, vol.65, No.1, pp. 108-121, Jan.1977.

[6] S.M. Anlage, V.V. Talanov,A.R. Schwartz, "Principles of Near-Field Microwave Microscopy," January 2006, Journal of Scanning Probe Microscopy 1:207-245, DOI: 10.1007/978-0-387-28668-6-8.

[7] Z.Chu, L.Zheng, K.Lai, "Microwave Microscopy and Its Applications," Ann. Rev.Mater.Res.2020.50:1.1–1.2, doi.org/10.1146/annurev-matsci-081519-011844.

[8] Michaels Faraday's Iron fillings, The Royal Institution, https://www.rigb.org/explore-science/explore/collection/michael-faradays-iron-filings.

[9] J.Ch. Bolomey, et al., "Rapid Near-Field Antenna Testing Via Arrays of Modulated Scattering Probes", in IEEE Trans. Ant. and Propag., vol. 36, no. 6, pp. 804-814, June 1988.

[10] M. Sierra Castaner and L.J. Foged, "Post-processing Techniques in Antenna Meausrements", Sci.Tech Publishing, IET, London, 2019.

[11] D. Iams, "Phase-front Plotter for Centimeter Waves", RCA Review, Jan. 1947, pp. 270-276.

[12] R.M. Barret, M.H. Barnes, "Automatic Antenna Wavefront Plotter Numerical Calculation and Experimental Verification", Electronics,Vol. 25, pp.121-125, Jan.1952.

[13] A. Yaghjiyan, "An Overview of Near-Field Antenna Measurements", IEEE Trans. Ant; and Propag;, Vol.AP-34 No.1, pp30-44, Jan.1986.

[14] J.H. Richmond, Vol.3, 1955, pp. 13-15nd, ". H. Richmond, "A Modulated Scattering Technique for Measurement of Field Distributions," in IRE Transactions on Microwave Theory and Techniques", vol. 3, no. 4, pp. 13-15, July 1955, doi: 10.1109/TMTT.1955.1124953.

[15] J.Ch. Bolomey and F. Gardiol, "Engineering Applications of the Modulated Scatterer Technique", Artech House, London, 2001.

[16] J. Peng, S. Jia, J. Bian, S. Zhang, J. Liu, X. Zhou, "Recent Progress on Electromagnetic Field", Sensors 2019, doi:10.3390/s19132860.

[17] A. Sârbu, P. Bechet, S. Miclăuș "Limitations of using electro-optical probes for the measurement of the electromagnetic field emitted by the new generations of wireless communication devices", IOP Conf. Series: Materials Science and Engineering, 1254 (2022) 012022, doi 10.1088/1757-899X/1254/1/012022.

[18] D.J. Lee and J.F. Whitaker, "An optical-fiber-scale electro-optic probe for minimally invasive high-frequency field sensing", 22 December 2008 / Vol. 16, No. 26 / OPTICS EXPRESS 21587.

[19] C.L. Holloway, et al., "Atom-Based RF Electric Field Metrology: From Self-Calibrated Measurements to Subwavelength and Near-Field Imaging", IEEE Trans. Electromagnetic Compatibility, Vol. 59, No. 2, pp. 717-728, April 2017, doi: 10.1109/TEMC.2016.2644616.

[20] J. Yuan, W. Yang, M. Jing, H. Zhang, Y. Jiao, W. Li, L. Zhang, L. Xiao, and S. Jia, "Quantum sensing of microwave electric fields based on Rydberg atoms", arXiv:2401.01655v1 [physics.atom-ph] 3 Jan 2024.

[21] B. Yang, M.M. Dong, W.H. He, Y. Liu, C.M. Feng, Y.J. Wang, G.X. Du, "Using Diamond Quantum Magnetometer to Characterize Near-Field Distribution of Patch Antenna", in IEEE Transactions on Microwave Theory and Techniques, vol. 67, no. 6, pp. 2451-2460, June 2019, doi: 10.1109/TMTT.2019.2908399.

[22] B. Yang, G. Du, Y. Dong, G. Liu, Z. Hu, Y. Wang, "Non-Invasive Imaging Method of Microwave Near Field Based on Solid State Quantum Sensing", IEEE Trans. Microwave Theory and Techniques, Vol. 66, No. 5, May 2018, doi:10.1109/TMTT.2018.2812204.

[23] Y. Shi, K. Ouyang, W. Ren, W. L. Meng, Cao, Z. Xue, M. Shi, "Near-field antenna measurement based on Rydberg-atom probe", Optics Express, Vol. 31, No. 12 / 5 Jun 2023 / Optics Express 18931, doi.org/10.1364/OE.485962.

[24] D. Booth, K. Nickerson, S. Bohaichuk, J. Erskine, J. P. Shaffer, "Rydberg Atomic Electrometry: A Near-Field Technology for Complete Far-Field Imaging in Seconds?", 2022 IEEE/MTT-S International Microwave Symposium - IMS 2022, Denver, CO, USA, 2022, pp. 853-855, doi: 10.1109/IMS37962.2022.9865387.

[25] F. Behague et al., "Minimally Invasive Optical Sensors for Microwave Electric-field Exposure Measurements", Journ. Opt. Microsystems, 2-7 April 2021, DOI: 10.1117/1.JOM.1.2.020902.

[26] A. Arboleya et al., "Freehand System for Probe-Fed Antenna Diagnostics by Means of Amplitude-Only Acquisitions", in IEEE Transactions on Instrumentation and Measurement, vol. 73, pp. 1-4, 2024, Art no. 8002004, doi: 10.1109/TIM.2024.3369150.

[27] J.Rioult et al., "Autonomous electromagnetic mapping system in augmented reality", 2019

Int. Symp. on EMC, Barcelona, pp. 138-143, doi:10.1109/EMCEurope.2019.8872055.

[28] G. Collignon Y. Michel, F. Robin, J.Ch. Bolomey, "Microwave Field Mapping for Large Antennas", Microwave Journal, Vol 25, n°129-132, pp 45-53, December 1982.

[29] C. Chekroun, D. Herrick, Y. Michel, R. Pauchard, P. Vidal, "Radant: New method of electronic scanning", Microwave Journal, Vol 24, n°2, pp 45-53, February 1981.

[30] R. Park, "Radant lens: alternative to expansive Phased arrays", Microwave Journal, Vol 24, n°9, pp 101-105, September 1981.

[31] G. Peronnet, Ch. Pichot, J .Ch. Bolomey, L. Jofre, A. Izadnegahdar, C. Szeles, Y. Michel, J.L. Guerquin-Kern, M. Gautherie, "A Microwave Diffraction Tomography System for Biomedical Applications", 1983 13th European Microwave Conference, Nurnberg, Germany, 1983, pp. 529-533, doi: 10.1109/EUMA.1983.333285.

[32] J.Ch. Bolomey, G. Cottard, B.J. Cown, "On-Line Transverse Control of Materials by Means of Microwave Imaging Techniques", Materials Research Society Symp. Proc. Vol. 189, pp 49-53. @1991.

[33] J.Ch. Bolomey, "New concepts for microwave sensing", SPIE, Proc. Reprint., Vol. 2275, July 1994.

[34] J.Ch. Bolomey, G. Cottard, P. Berthaud, A. Lemaitre, J.F. Portala, "Microwave On-Line Measurements on Conveyed Products Application to Paper And Wood Industries," Materials Research Society Symp. Proc. Vol. 347, pp. 161-168. 1994.

[35] J.Ch. Bolomey and Ch. Pichot, "Microwave Tomography: From Theory to Practical Imaging Systems," International Journal of Imaging Systems and Technology

[36] R. Zoughi, "Microwave Real-Time and High-resolution Imaging System Development for NDT Applications: A Chronology," ASNT Journal, Vol.81, No.9, 2023 https://doi.org/10.32548/2023.me-04349.

[37] N. V. Shahmirzadi, N. K. Nikolova, C.H. Chen, "Interconnect for Dense Electronically Scanned Antenna Array Using High-Speed Vertical Connector," Sensors 2023, 23, 8596, doi.org/10.3390/s23208596.

[38] T. Rubæk, X. Zhurbenko, "Phantom experiments with a microwave imaging system for breast-cancer screening," In Proc. 3rd European Conference on Antennas and Propagation, pp. 2950-2954, EuCAP 2009.

[39] J.Ch. Bolomey, L. Jofre, "Three Decades of Active Microwave Imaging Achievements, Difficulties and Future Challenges." 2010 IEEE International Conference on Wireless Information Technology and Systems. https://doi.org/10.1109/ICWITS.2010.5611904.

[40] H. Tao, E.A. Kadlec, A.C. Strikwerda, K. Fan, W.J. Padilla, R.D. Averitt, E.A. Shaner, X. Zhang, "Microwave and Terahertz wave sensing with metamaterials, 2011 OSA, OPTICS EXPRESS, Vol. 19, No. 22, pp. 21620-21625.

[41] Y. Xie, X. Fan, Y. Chen, J.D. Wilson, R.N. Simons, J. Q. Xiao, "A subwavelength resolution microwave/6.3 GHz camera based on a metamaterial absorber," Sci. Rep. 7, 40490; doi: 10.1038/srep40490 (2017).

[42] D. Shrekenhamer, W. Xu, S. Venkatesh, D. Schurig, S. Sonkusale, W. J. Padilla, "Experimental Realization of a Metamaterial Detector Focal Plane Array," Physical Review Letters, October 2012, doi: 10.1103/PhysRevLett.109.177401.

[43] Z. Baghdasaryan, A. Babajanyan, B. Friedman, K. Lee, "Characterization of interaction phenomena of electromagnetic waves with metamaterials via microwave near-field visualization technique," 10.1038/s41598-023-45665-4.

[44] P. Mei, G.F. Pedersen, Q. Liu, X. Q. Lin, S. Zhang, "An Overview of Metamaterial Absorbers and Their Applications on Antenna", Proc. 2022 PhotonIcs Electromagnetics Research Symposium (PIERS), pp 1053-1060, Hangzhou, China, 25-27 April 2022, doi: 10.1109/PIERS55526.2022.9792666.

[45] L. J. Foged, M. Sierra-Castañer and L. Scialacqua, "Facility comparison campaigns within EurAPP", Proceedings of the 5th European Conference on Antennas and Propagation (EUCAP), Rome, Italy, 2011, pp. 2541-2545.

[46] L. Scialacqua, F. Mioc, J. Zhang, L. J. Foged, M. Sierra-Castañer, EuCAP 2011,"Antenna measurement intercomparison campaigns in the framework of the European Association of Antennas and Propagation", 2013 Proceedings of the International Symposium on Antennas and Propagation, Nanjing, China, 2013, pp. 290-293.

[47] J. Araque, G. Vecchi. "Improved-accuracy source reconstruction on arbitrary 3-D surfaces", IEEE Antennas and Wireless Propagation Letters, 8:1046–1049, 2009.

[48] L. J. Foged, L. Scialacqua, P. Iversen and E. Szpindor, "Detection and suppression of scattered fields from coplanar micro-probe and positioner in millimeter wave on-chip antenna measurements," 2016 International Symposium on Antennas and Propagation (ISAP), Okinawa, Japan, 2016, pp. 126-127.

[49] Yuri Álvarez, Fernando Las-Heras, Marcos R. Pino, "Antenna Diagnostics Using Phaseless NF Information," AUTOMATIKA 53(2012) 1, 49–55 49, doi: 10.7305/automatika.53-1.138

[50] J. Laviada and F. Las-Heras, "Phaseless Antenna Measurement on Non-Redundant Sample Points via Leith-Upatnieks Holography," in IEEE Transactions on Antennas and Propagation, vol. 61, no. 8, pp. 4036-4044, Aug. 2013, doi: 10.1109/TAP.2013.2262669.

[51] B. Fuchs, M. Mattes, S. Rondineau and L. Le Coq, "Phaseless Near-Field Antenna Measurements from Two Surface Scans — Numerical and Experimental Investigations," in IEEE Transactions on Antennas and Propagation, vol. 68, no. 3, pp. 2315-2322, March 2020, doi: 10.1109/TAP.2019.2938744.

[52] F. Rodríguez Varela, J. Fernandez Álvarez, B. Galocha Iragüen, M. Sierra Castañer and O. Breinbjerg, "Numerical

and Experimental Investigation of Phaseless Spherical Near-Field Antenna Measurements," in IEEE Transactions on Antennas and Propagation, vol. 69, no. 12, pp. 8830-8841, Dec. 2021, doi: 10.1109/TAP.2021.3090846.

[53] Y. Alvarez, F. Las-Heras and M. R. Pino, "Reconstruction of Equivalent Currents Distribution Over Arbitrary Three-Dimensional Surfaces Based on Integral Equation Algorithms", in IEEE Transactions on Antennas and Propagation, vol. 55, no. 12, pp. 3460-3468, Dec. 2007, doi: 10.1109/TAP.2007.910316

[54] A.M. Vural, D.K. Cheng, "A Light-Modulated Scattering Technique for Diffraction Field Measurements," RADIO SCIENCE Journal of Research, NBSJUSNC- URSI Vol. 68D No.4, pp. 355-362, April 1964

[55] G. Hygate, "A modulated scatterer for measuring microwave fields," IEE Colloquium on Calibration of Antennas for Close Range Measurements, London, UK, 1990, pp. 3/1-3/4.

[56] Liao Ma , Ning Leng , Ming Jin, Ming Bai, "High-efficiency Diagnosis of Antenna Radiation Characteristics Based on Scanning Optic-Induced Plasma Scattering Technology,' IEEE Trans. Ant. Propag., Vol. 71, No. 4, April 2023.

[57] L. Ma, N. Leng, M. Jin, M. Bai, "Real-Time Imaging of Electromagnetic Fields," Vol.30, No.12, 6 Jun 2022, Optics Express 20431, https://doi.org/10.1364/OE.461137.

[58] N. Leng, L. Ma, Z. Liang, M. Bai, "Measurement of Very-Near-Field Distribution of Onboard Antenna Using Scanning Optic-Induced Plasma Scattering Technology," 2025 19th European Conference on Antennas and Propagation (EuCAP).

[59] N. Leng, L. Ma, P. Ou, M. Bai, "A Microwave Holographic Imaging Method by Photo-induced Plasma Scanning," 2023 PhotonIcs Electromagnetics Research Symposium (PIERS), Prague, doi: 10.1109/PIERS59004.2023.10221345.

[60] N. Prajapti et al., "Synthetic Aperture RF Reception using Rydberg Atoms," 2023 IEEE ICASSPW, doi:10.1109/ICASSPW59220.2023.10193367.

[61] C.L. Holloway et al., "Overview of Rydberg Atom-Based Sensors/Receivers for the Measurement of Electric Fields, Power, Voltage, and Modulated Signals," in Antenna and Array Technologies for Future Wireless Ecosystems, First Edition, Y. Jay Guo and R.W. Ziolkowski Eds., 2022 The Institute of Electrical and Electronics Engineers, Inc. Published 2022 by John Wiley Sons, Inc.

[62] Amarloo et al., "Vapor Cells for Imaging of Electromagnetic Fields," International Patent WO 2021/102555 A1, June 2021, Quantum Valleys Ideas Lab., Waterloo (CA).

[63] Amarloo et al., "Photonic Crystal Vapor Cells for Imaging of Electromagnetic Fields," U.S. Patent 2021/0156898 A1, May 2021, Quantum Valley Ideas Laboratories, Waterloo (CA).

[64] V. Aksyuk, et al., "Photonic Rydberg Atom Radio Frequency Receiver and Measuring a Radio Frequency Electric Field," U.S. Patent 2022/0390496 A1, Dec. 2022.

[65] C.L. Holloway, M. Simons, "Atomic Vapor Cell and Making an Atomic Vapor Cell," U.S. Patent 20220018914-A1, Jan. 2022, and C.L. Holloway et al., "Atomic Vapor Cell and Making an Atomic Vapor Cell," U.S. Patent 11,879,952 B2, Jan. 2024.

[66] L. Basso, P. Kehayias, J. Henshaw, G. Joshi, M.P. Lilly, M.B. Jordan and A.M. Mounce, "Wide-field microwave magnetic field imaging with nitrogen-vacancy centers in diamond", arXiv:2409.16528v1 [physics.app-ph] 25 Sep 2024.

[67] X. Jia, Y. Qin, Z. Luo, S. Zhu,X. Li, H. Guo, "Near-Field Microwave Imaging Method of Monopole Antennas Based on Nitrogen-Vacancy Centers in Diamond", Micromachines, Vol. 15, n°6, p 679, May 2024.

[68] https://www.emcfastpass.com/test-equipment/shop/near-field-scanners/emscan-rfx2-benchtop-antenna-scanner/

[69] S. Wane et al., "High Resolution Spintronics Probe-Array Technology Solutions for Very Near-Field Scanning", 2021 IEEE CAMA Conference, Antibes Juan-les-Pins, France, 2021, pp. 241-246, doi: 10.1109/CAMA 49227.2021.9703656.

[70] J.S. Previti, "EMSCAN: A tool to measure emissions from printed circuit packs", EMC Technology, vol. 8, pp. 3-5, NOV. 1989.

[71] "Real-time EMC and EMI diagnostic tool: Test ultra-high speed ($>$ 2GHz) PCBs in real-time on your lab-bench", www.emscan.com

[72] Rezvan Rafiee Alavi, Ali Kiaee, Ruska Patton, Rashid Mirzavand, Pedram Mousavi, "High Resolution VNF measurement technique to detect defected vias in SIW structures; Comparison between single probe and fast electronically switched probe array results". www.emscan.com.

[73] R. R. Alavi, A. Kiaee, R. Mirzavand, R. Patton, P. Mousavi, J. Ch. Bolomey, "Extraction of Via Defects from Very-Near-Field Measurement and Source Reconstruction Method," 2nd URSI AT-RASC, Gran Canaria, 28 May – 1 June 2018.

[74] A. Kiaee, R. R. Alavi, M. M. Honari, R. Mirzavand and P. Mousavi, "Ground de-embedded source reconstruction using a planar array of H field probes," IEEE Int. Symp. Antennas Propagation USNC/URSI National Radio Science Meeting, San Diego, 2017, pp. 133-134.

[75] M. Kanda, "Standard Probes for Electromagnetic Field Measurements," IEEE Transactions Antennas and Propagation, Vol. 41, No. 10, pp. 1349-1364, October 1993.

[76] J.J. Laurin, Z. Ouardhiri and J. Colinas, "Near-field imaging of radiated emission sources on printed-circuit boards," 2001 IEEE EMC International Symposium. Symposium Record. International Symposium on Electromagnetic Compatibility (Cat. No.01CH37161), Montreal, QC, Canada, 2001, pp. 368-373 vol.1, doi: 10.1109/ISEMC.2001.950665.

[77] T. P. Budka, S. D. Waclawik and G. M. Rebeiz, "A coaxial 0.5-18 GHz near electric field measurement system for planar microwave circuits using integrated probes," in IEEE Transactions on Microwave Theory and Techniques, vol. 44, no. 12, pp. 2174-2184, Dec. 1996, doi: 10.1109/22.556445

[78] J.J. Laurin, J.F. Zürcher, and F.E. Gardiol, "Near-Field Diagnostics of Small Printed Antennas Using the Equivalent Magnetic Current Approach," IEEE Transactions on Antennas and Propagation, Vol. 49, No. 5, pp. 814-828, May 2001.

[79] Z. Chu, L. Zheng,K. Lai, "Microwave Microscopy and Its Applications", An. Review Mat. Res., ARjats.cls, March 16, 2020.

[80] A. Imtiaz, T.M. Wallis, P. Kabos,"Near-Field Scanning Microwave Microscopy," IEEE Microwave Magazine, pp.52-64, Jan/Feb.2014, doi: 10.1109/MMM.2013.2288711

[81] P. Polovodov et al., "Electromagnetic Modeling in Near-Field Scanning Microwave Microscopy Highlighting Limitations in Spatial and Electrical Resolutions," 2018 IEEE MTT-S International Conference on Numerical Electromagnetic and Multiphysics Modeling and Optimization (NEMO), Reykjavik, Iceland, 2018, pp. 1-4, doi: 10.1109/NEMO.2018.8503487.

[82] S. K. Dutta, C. P. Vlahacos, D. E. Steinhauer, Ashfaq S. Thanawalla, B. J. Feenstra, F. C. Wellstood, S.M. Anlage, "Imaging Microwave Electric Fields Using a Near-Field Scanning Microwave Microscope," arXiv:cond-mat/9811140v1 10 Nov 1998, 10.1063/1.123137

[83] Kasra Payandehjoo, Ruska Patton, "De-embeding the effect of a printed array of probes on planar very-near-field measurements," 2014 IEEE Conference on Antenna Measurements and Applications (CAMA), Antibes Juan-les-Pins, France, 2014, pp. 1-4, doi: 10.1109/CAMA.2014.7003433.

[84] W.B. Kock and F.K. Harvey, "A photographic method for displaying sound wave and microwave space patterns," in The Bell System Technical Journal, vol. 30, no. 3, pp. 564-587, July 1951, doi: 10.1002/j.1538-7305.1951.tb03670.x.

[85] A.I. Petrariu and E. Coca, "Real-Time 3D Near-Field Visualization Using LED Field Sensors," 2016 IEEE 22nd Int. Symp. for Design and Technology in Electronic Packaging (SIITME), Oradea, Romania, 978-1-5090-4445-0/16.

[86] T. Hasegawa, "A New Method of Observing Electro-Magnetic Fields at High Frequencies by Use of Test Paper", Bull. Yamagata Univ. IV, Japan 1955.

[87] K. Iizuka, "A method for Photographing Microwaves with a polaroid film" Div. Engineering and Applied Physics, Harvard Univ. Cambridge, Mass., Technical Report 558, March 1968.

[88] C.F. Augustine, "Field Detector Works in Real Time: Liquid Crystals Provide Instant Display of Microwave Intensity in Color", Electronics June 24, pp. 118-122, 1968.

[89] K. Iizuka, "Mapping of Electromagnetic Fields by Photochemical Reaction", Electronics Letters, Vol.4, 1968.

[90] P.A. Dar, "Infrared Thermography for Characterization of Microwave Fields: A Brief Overview and Review", 2019 JETIR March 2019, Volume 6, Issue3, www.jetir.org (ISSN-2349-5162).

[91] R.M. Sega, "Infrared Detection of Microwave Induced Surface Currents on Flat Plates", United States Ar Force Academy, RADC-TR-82, Final Technical Report, December 1982.

[92] C. Corsi, "History highlights and future trends of infrared sensors, Tutorial Review," Journal of Modern Optics Vol. 57, No. 18, 20 October 2010, 1663–1686, DOI: 10.1080/09500341003693011.

[93] M. Kimata, "Uncooled Infrared Focal Plane Arrays," IEEJ Trans 2018; 13: 4–12 doi:10.1002/tee.22563

[94] R. Usamentiaga, P. Venegas, J. Guerediaga, L. Vega, J. Molleda and F.G. Bulnes, "Infrared Thermography for Temperature Measurement and Non-Destructive Testing,'Sensors 2014, 14, 12305-12348; doi:10.3390/s140712305

[95] B.B. Lahiri, S. Bagavathiappan, T. Jayakumar, John Philip, "Medical applications of infrared thermography: A review," Infrared Physics Technology, 55 (2012)221-235, http://dx.doi.org/10.1016/j.infrared.2012.03.007.

[96] P.A. Dragana, B. Livada,, "Infrared Thermography for Characterization of Microwave Fields: A Brief Overview and Review," 2019 JETIR March 2019, Volume 6, Issue3, www.jetir.org (ISSN-2349-5162).

[97] L.G. Gregoris, K. Iizuka, "Thermography in a microwave regime," Applied Optics. vol.14, 1975.

[98] J. Will, J. Norgard, C. Stubenrauch, M. Seifert, "Infrared Imaging Techniques for the Measurement of Complex Near-field Antenna Patterns Double Plane Measurement," Qirt 96 - Eurotherm Series 50, http://Dx.Doi.Org/10.21611/Qirt.1996.011

[99] J.D. Norgard,"Infrared/microwave correlation measurements," Opt. Eng., 1994, 33, pp. 85-96

[100] Parvaiz Ahmad Dar, " Infrared Thermography for Characterization of Microwave Fields: A Brief Overview and Review," 2019 JETIR March 2019, Volume 6, Issue3, www.jetir.org (ISSN-2349-5162).

[101] K. Muzaffar et al., "Fault detection of antenna arrays using infrared thermography," Infrared Physics Technology 71 (2015) 464–468.

[102] D. Balageas and P. Levesque, "EMIR: a Photothermal Tool for Electromagnetic Phenomena Characterization," Revue Générale de Thermique, 37(8):725-739, Sept. 1998, doi: 10.1016/S0035-3159(98)80050-0.

[103] R.M. Sega, C.A. Benckelman, "Measurement of Antenna Patterns at 94 GHz Using Infrared Detection", Millimeter Wave Technology III, SPIE Vol. 544, April 1985.

[104] O. Breitenstein, M. Langenkamp, F. Altmann D. Katzer, A. Lindner, H. Eggers, "Microscopic lock-in thermography investigation of leakage sites in integrated circuits," Rev.

Sci. Instrum., Vol. 71, No. 11, pp. 4155-4160, November 2000.

[105] D.L. Balageas, P. Levesque, A. Déom, "Characterization of electromagnetic fields using lock-in IR thermography", Thermosense XV, SPIE, vol. 1933, pp. 274-285, 1993.

[106] K. Muzaffar, K.Chatterjee, L.I. Giri, S. Koul, S. Tuli, "Modelling and Analysis of Power Distribution of Electromagnetic Waves on Plane Surfaces Using Lock-in IR Thermography," J. Nondestruct Eval (2017) 36:60, doi: 10.1007/s10921-017-0439-z.

[107] J. Lundgren, M. Gustafsson, D. Sjöberg, M. Nilsson, "IR and Metasurface Based mm-wave Camera", Appl. Phys. Lett. 118, 184104 (2021); doi: 10.1063/5.0047315 https://doi.org/10.1063/5.0047315.

[108] B.A.P. Nel, A. K. Skrivervik, J.Lundgren, M. Gustafsson, "Impact of Metasurface Element Designs on Infrared-Based Antenna Near-Field Measurements," European Microwave Conference on Antennas and Propagation (EuCAP2025), Stockholm, April 7-11, 2025.

[109] F. Lestini et al., "Epidermal RFID-Based Thermal Monitoring Sheet for Microwave Hyperthermia", IEEE Trans. on Electromag, RF and Microwaves in Medicine and Biology, Vol. 7, No. 4, pp. Dec. 2023.

[110] F. Lestini, G. Marrocco, C. Occhiuzzi, "Varactor-Tunable RFID-Based Wireless Programmable Frequency Selective Surface as a Smart Shield for Implanted Medical Devices," European Microwave Conference on Antennas and Propagation (EuCAP2025), Stockholm, April 7-11, 2025.

[111] K.Muzaffar, S. Tuli and S. Koul, "Infrared thermography for electromagnetic field pattern recognition", IEEE MTT-S International Microwave and RF Conference, New Delhi, India, 2013, pp. 1-4, doi: 10.1109/IMaRC.2013.6777742.

[112] K. Muzaffar et al., "Fault detection of antenna arrays using infrared thermography", Infrared Physics and Technology 71 (2015) 464–468.

[113] Don W. Metzger, J.D. Norgard and R.M. Sega, "Near-field Patterns from Pyramidal Horn Antennas: Numerical Calculation and Experimental Verification", IEEE Trans. Electromagnetic Compatibility, Vol. 33, No. 3, 188-199, August 1991.

[114] C.F. Stubenrauch et al., "Far-field antenna patterns determined from infrared holograms", Proc. of 1999 IEEE Symp. Antenna Propagat. Soc., Orlando, FL.

[115] D. Prost, F. Issac, F. Lemaître and J. P. Parmantier, "Infrared thermography of microwave electromagnetic fields", International Symposium on Electromagnetic Compatibility - EMC Europe, Rome, Italy, 2012, pp. 1-4, doi:10.1109/EMCEurope.2012.6396669.

[116] D. Prost, F. Issac and M. Romier, "Imaging electric and magnetic near field of radiating structures by infrared thermography", 2019 International Symposium on Electromagnetic Compatibility - EMC Europe, Barcelona, Spain, Nov. 2019, pp. 311-314, doi: 10.1109/EMCEurope.2019.8872116.hy, HAL Id: hal-02364926.

[117] J. E. Will, J. Norgard, C. Stubenrauch, M. Seifert , "Complex near-field antenna measurements using infrared (IR) thermograms", 1996 Symp. on Ant. Techno. and Appl. Electromag., Montreal, QC, Canada, 1996, pp.125-128, doi: 10.21611/Qirt.1996.011.

[118]] J.M. Gonzalez, A. Aguasca and J. Romeu, "Infrared thermograms applied to near-field testing," ELECTRONICS LETTERS 27th May 1999 Vol. 35 No. 11, pp. 885-886.

[119] C. Baer, K. Orend, B. Hattenhorst, T. Musch, "Field Representation Microwave Thermography Utilizing Lossy Microwave Design Materials," Sensors, 2021, 21, 4830. https://doi.org/10.3390/s21144830.

[120] S. Faure, J.F. Bobo, D. Prost, F.Issac, J.Carey,"Electromagnetic Field Intensity Imaging by Thermofluorescence in the Visible Range", Phys. Rev. Applied 11, 054084, 2019.

[121] R. Flor, S. Fauré, J.F. François Bobo, D. Prost, "Fluorescence Thermography for High-Resolution Characterization of Transmitarray Antenna in X Band," European Microwave Conference on Antennas and Propagation (EuCAP2025), Stockholm, April 7-11, 2025.

[122] R. Flor, S. Fauré, J.F. François Bobo, D. Prost, "Fluorescence Thermography for High-Resolution Characterization of Transmitarray Antenna in X Band," European Microwave Conference on Antennas and Propagation (EuCAP2025), Stockholm, April 7-11, 2025.

[123] D. Wang, H.F. Wen, X. Li, Y. Jin, W. Hao, Z. Gao, Y. Liu, Z. Li, H. Guo, Z. Ma, J. Tang, and J. Liu, "Toward Characterizing 3-D Microwave Field With Microscale Resolution Using Nitrogen-Vacancy Centers in Diamond," IEEE Transactions On Instrumentation And Measurement, Vol. 72, 2023 8006307 (chip)

[124] Patrick Appel, Marc Ganzhorn, Elke Neu and Patrick Maletinsky, "Nanoscale microwave imaging with a single electron spin in diamond," New J. Phys. 17 (2015) 112001 doi:10.1088/1367-2630/17/11/112001.

[125] L. Shao, et al , "Wide-Field Optical Microscopy of Microwave Fields Using Nitrogen-Vacancy Centers in Diamonds", Adv. Optical Mater., 2016,4,1075–1080, doi: 10.1002/adom.201600039.

[126] B.Yang, M.M. Dong, W.H.He, Y.Liu, C.M.Feng, Y.J.Wang,G.X. Du, "Using Diamond Quantum Magnetometer to Characterize Near-Field Distribution of Patch Antenna", IEEE Trans. Microwave Theory and Techniques, Vol.67, No. 6, June 2019

[127] B. Yang, et al. "Noninvasive Imaging Method of Microwave Near Field Based on Solid-State Quantum Sensing", in IEEE Trans. MTT, vol. 66, no. 5, pp. 2276-2283, May 2018.

[128] X. Jia, Y. Qin, Z. Luo, S. Zhu,X. Li, H. Guo, "Near-Field Microwave Imaging Method of Monopole Antennas Based on Nitrogen-Vacancy Centers in Diamond," Micromachines, Vol. 15, n°6, p 679, May 2024.

[129] H. Lee, S. Jeon, B. Friedman, K. Lee, "Simultaneous Imaging of Magnetic Field and Temperature Distributions by Magneto Optical Indicator Microscopy," Scientific Reports — 7:43804 — 02 March 2017 I DOI: 10.1038/srep43804

[130] M.P. Path, J. McCord, "Quantitative Magnetooptical Analysis Using Indicator Films for The Detection of Magnetic Field Distributions, Temperature, and Electrical Currents," Scientific Reports (2024) 14:25459, https://doi.org/10.1038/s41598-024-74684-y.

[131] H. Lee, S. Arakelyan, B. Friedman et al. Temperature and microwave near field imaging by thermo-elastic optical indicator microscopy. Sci Rep 6, 39696 (2016). doi: 10.1038/srep39696.

[132] Z.A. Baghdasaryan, "Imaging of Microwave Near-field Distribution of GPS Patch Antenna," Proceedings of the Yerevan State University Physic. and Math. Sc. (2022), 56(2), p. 66–73. https://doi.org/10.46991/PYSU:A/2022.56.2.066.

[133] Z. Baghdasaryan, A. Babajanyan, B. Friedman, K.Lee, "Characterization of Interaction Phenomena of Electromagnetic Waves with Metamaterials via Microwave Near field Visualization Technique," natureportfolio, ScientificReports (2023)13:18457, https://doi.org/10.1038/s41598-023-45665-4.

[134] K.Yazawa, D. Kendig, P.E. Raad, P.L. Komarov, A. Shakouri, "Understanding the Thermo-Reactance Coefficient for High Resolution Thermal Imaging of Microelectronic Devices," Electronics Cooling, March 8, 2013.

[135] M. Farzaneh,K. Maize,D. Lüerßen, J.A. Summers, P.M. Mayer, P.E. Raad,K.P. Pipe, A. Shakouri, R.J. Ram, J.A. Hudgings, "CCD-based thermoreflectance microscopy: principles and applications," J. Phys. D: Appl. Phys. 42 (2009) 143001 (20pp) doi:10.1088/0022 3727/42/14/143001

[136] D. Fournier, C. Filloy, S. Holé, J.P. Roger and G. Tessie, "Nano and microscale thermal transport experimental measurements" J. Phys. IV France 125 (2005) 493-498, EDP Sciences, Les Ulis, doi: 10.1051/jp4:2005125115

[137] A. Ziabari, M. Parsa, Y. Xuan, J.H. Bahk, K. Yazawa, F. Xavier Alvarez, A. Shakouri, "Far-field thermal imaging below diffraction limit", Optics Express, Vol. 28, No. 5, 2 March 2020.

[138] T. Favaloro, J.-H. Bahk, and A. Shakouri, "Characterization of the temperature dependence of the thermo-reflectance coefficient for conductive thin films," Rev. Sci. Instrum. 86, 024903 (2015). https://doi.org/10.1063/1.4907354

[139] G. Tessier M. Bardoux C. Filloy C. Boué D. Fournier, (2007),"High resolution thermal imaging inside integrated circuits", Sensor Review, Vol. 27 Issue 4 pp. 291 - 297 http://dx.doi.org/10.1108/02602280710821425.

[140] S. Wane et al., "Combined Thermo-Reflectance and Thin-Film Coating in Near-Field Imaging of Chip-Package-PCB-Antenna Modules for Industrial-Testing and Failure Analysis," 2023 IEEE Texas Symposium on Wireless and Microwave Circuits and Systems (WMCS), doi: 10.1109/WMCS58822.2023.10194284.

[141] M. Shakouri, S.Wane, "An Innovative Non-invasive Analysis and Testing of Advanced Packaging Systems such as Antenna-in-Package and Antenna-on-Chip," 2023 IEEE CAMA, Genova, Italy, Nov. 2023.

[142] M. Shakouri, S. Wane, "Advances in Thermal Analysis and Over-The-Air Electromagnetic Analysis of Advanced Microwave Devices and Front-End-Modules," IMS 2024, Half-day workshop, 16-21 June, Washington, https://microsanj.com/join-us-in-washington-dc-for-ims-2024/

[143] A.Alu and N. Engheta, "Cloaking a Sensor," Phys. Rev. Lett. 102, 233901, doi: 10.1103/PhysRevLett.102.23390.

[144] Pradnya A. Gajbhiye, Satya P. Singh, Madan Kumar Sharma, "A comprehensive review of AI and machine learning techniques in antenna design optimization and measurement". Discover Electronics. June 2025. https://doi.org/10.1007/s44291-025-00084-9.

[145] M. Sierra-Castañer, "Review of Recent Advances and Future Challenges in Antenna Measurement". Applied Computational Electromagnetics Society. Express Journal. Feb. 2016, Vol. 1 No. 2. Pag. 64-67.